

Cite this: *Chem. Sci.*, 2024, 15, 11875

All publication charges for this article have been paid for by the Royal Society of Chemistry

Kinetics of sulfur-transfer from titanocene (poly)sulfides to sulfenyl chlorides: rapid metal-assisted concerted substitution†‡

Pedro H. Helou de Oliveira,^a Patrick J. Boaler,^a Guoxiong Hua,^b Nathan M. West,^c Robert T. Hembre,^c Jonathan M. Penney,^d Malik H. Al-Afyouni,^d J. Derek Woollins,^e Andrés García-Domínguez^{§*a} and Guy C. Lloyd-Jones^{§*a}

The kinetics of sulfur transfer from titanocene (poly)sulfides (^RCp₂TiS₅, Cp₂TiS₄CMe₂, Cp₂Ti(SAR)₂, Cp₂TiCl(SAR)) to sulfenyl chlorides (S₂Cl₂, RSCl) have been investigated by a combination of stopped-flow UV-Vis/NMR reaction monitoring, titration assays, numerical kinetic modelling and KS-DFT calculations. The reactions are rapid, proceeding to completion over timescales of milliseconds to minutes, via a sequence of two S–S bond-forming steps (*k*₁, *k*₂). The archetypal polysulfides Cp₂TiS₅ (**1a**) and Cp₂TiS₄C(Me₂) (**2a**) react with disulfur dichloride (S₂Cl₂) through rate-limiting intermolecular S–S bond formation (*k*₁) followed by a rapid intramolecular cyclization (*k*₂, with *k*₂ ≫ *k*₁ [RSCl]). The monofunctional sulfenyl chlorides (RSCl) studied herein react in two intermolecular S–S bond forming steps proceeding at similar rates (*k*₁ ≈ *k*₂). Reactions of titanocene bistiophenolates, Cp₂Ti(SAR)₂ (**5**), with both mono- and di-functional sulfenyl chlorides result in rapid accumulation of the monothiophenolate, Cp₂TiCl(SAR) (**6**) (*k*₁ > *k*₂). Across the range of reactants studied, the rates are relatively insensitive to changes in temperature and in the electronics of the sulfenyl chloride, moderately sensitive to the electronics of the titanocene (poly)sulfide ($\rho_{\text{Ti-(SAR)}} \approx -2.0$), and highly sensitive to the solvent polarity, with non-polar solvents (CS₂, CCl₄) leading to the slowest rates. The combined sensitivities are the result of a concerted, polarized and late transition state for the rate-limiting S–S bond forming step, accompanied by a large entropic penalty. Each substitution step {[Ti]–SR' + Cl–SR → [Ti]–Cl + RS–SR'} proceeds via titanium-assisted Cl–S cleavage to generate a transient pentacoordinate complex, Cl–[Cp₂TiX]–S(R')–SR, which then undergoes rapid Ti–S dissociation.

Received 26th April 2024
Accepted 16th June 2024

DOI: 10.1039/d4sc02737j

rsc.li/chemical-science

Introduction

Titanocene pentasulfide, Cp₂TiS₅ (**1a**, Scheme 1), is a bench-stable and easily handled pentasulfide dianion surrogate.^{1,2} Pentasulfide **1a**, and related polysulfides, (e.g. Cp₂TiS₄C(Me)₂, **2a**),^{2a} allow the selective preparation of sulfur homocycles (S_{*n*}),³ heterocycles (E₂S_{*n*}),⁴ and polysulfanes (R₂S_{*n*})⁵ from sulfenyl chlorides (S_{*x*}Cl₂, RS_{*x*}Cl). Titanocene bis and mono-thiolates, Cp₂Ti(SR)₂ and Cp₂TiCl(SR), are also efficient sulfide anion

surrogates.^{3c,6,7} These S–S bond-forming reactions generally proceed quantitatively under mild conditions (≤25 °C) making pentasulfide **1a** and analogues one of the central platforms for the synthesis of polysulfides.^{3d,8,9} Despite this widespread application, studies of the mechanism(s) of these sulfur transfer processes are scarce,^{2a,7a,10,11} and as far as we are aware the kinetics of the general process in Scheme 1 have not been investigated.

The reaction of pentasulfide **1a** with RSCl species is generally accepted to proceed in two steps, via a chlorotitanocene intermediate (**Int**), Scheme 1. Support for this includes the isolation of intermediates from the slow reactions of the sterically hindered sulfenyl chloride Ph₃CSCl with Cp₂TiS₄CMe₂ (**2a**) and with Cp₂TiS₄(cyclo-C₆H₁₀).^{7a} Münchow and Steudel proposed that nucleophilic attack by the chlorine atom in RSCl at the titanium atom opens the metallacycle (mechanism I).^{7a}

However, sulfur compounds can react ambiphilically and several alternative mechanisms can also be considered for the S–S bond forming steps. For example, concerted or step-wise S_N2-at-sulfur reactions are feasible,^{12–14} with **1a** acting as the nucleophile (mechanism II). Alternatively, the S–S bond

^aSchool of Chemistry, University of Edinburgh, David Brewster Road, Edinburgh, EH9 3FJ, UK. E-mail: v1agarc9@ed.ac.uk; guy.lloyd-jones@ed.ac.uk

^bSchool of Chemistry, University of St Andrews, North Haugh, St Andrews, KY16 9ST, UK

^cEastman Chemical Company, 200 S Wilcox Dr, Kingsport, Tennessee 37660, USA

^dFlexsys America L.P., 260 Springside Drive, Akron, OH 44333, USA

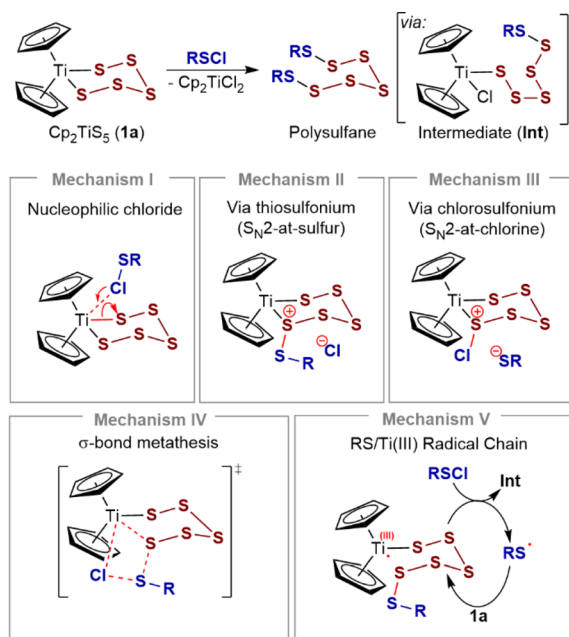
^eDepartment of Chemistry, Khalifa University, Abu Dhabi, UAE

† Dedicated to the memory of Prof. Dr Ralf Steudel (March 25, 1937–February 12, 2021) a life-long pioneer in the chemistry of sulfur.

‡ Electronic supplementary information (ESI) available. See DOI: <https://doi.org/10.1039/d4sc02737j>

§ AGD is a Royal Society University research fellow.





Scheme 1 Reaction of titanocene pentasulfide (**1a**) with sulfur(II) chlorides: general features and potential reaction mechanisms (I–V).

forming steps could involve formation of chlorosulfonium ions (mechanism III), concerted σ -bond metathesis (mechanism IV), or mechanisms involving sulfenyl radicals¹⁵ and Ti(III)¹⁶ chain carriers (mechanism V), or analogous chain processes. There is also the possibility that **1a** acts as a reservoir to reactive ring-opened species.¹⁷ Depending on specific kinetic parameters, these last two possibilities are unlikely to result in simple bimolecular kinetics (see ESI, Section S9†).

Results and discussion

Herein, we report on the kinetics of sulfur transfer from titanacyles (**1** and **2**) to sulfenyl chlorides S_2Cl_2 and to $RSCl$ reagents (**3** and **4**), including analysis of the effects of solvent and temperature on the rate. The experimental kinetic data are complemented with KS-DFT calculations to assess the feasibility of proposed reaction pathways and elucidate the key role of the titanocene in these nucleophilic substitutions. We also briefly report on the reactions of acyclic Ti-thiophenolates with S_2Cl_2 . The overall insight to the kinetics and mechanism allows the identification of parameters that can be used to tune the rate and selectivity.

Kinetics of the reaction of S_2Cl_2 with titanacycle **1a**

We began by investigating of the reaction of S_2Cl_2 with Cp_2TiS_5 (**1a**). Preliminary analysis by 1H NMR spectroscopy confirmed quantitative conversion within seconds in CH_2Cl_2 solution, accompanied by a characteristic change in colour from deep-red (Cp_2TiS_5 **1a**, λ_{max} 490 nm) to light-orange (Cp_2TiCl_2 , λ_{max} 393 nm).^{17b,c} Stopped-flow UV-Vis analysis (SF-UV) of the reactions of **1a**, at initial concentrations in the range 0.05–0.15 mM, with

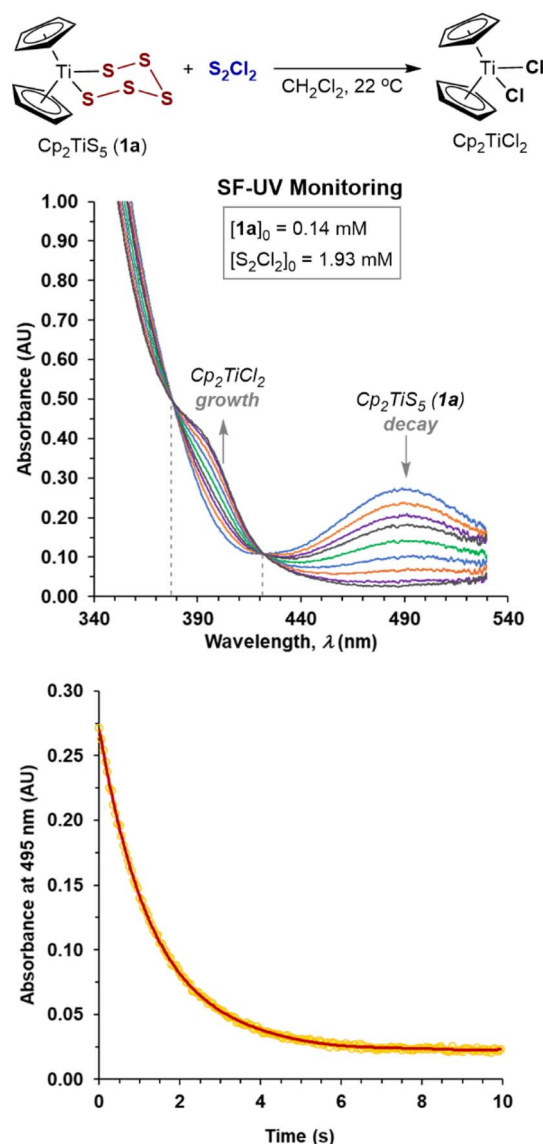


Fig. 1 Stopped-flow UV-Vis temporal evolution of spectra and exponential decay in absorbance of **1a** at 495 nm on reaction with excess S_2Cl_2 in CH_2Cl_2 at 22 °C.

a large excess of S_2Cl_2 (for conditions, see the ESI, Section S2†) were in agreement with pseudo first-order kinetics, with two clear isosbestic points ($\lambda = 378, 422$ nm, e.g. Fig. 1). The data correlated with the same exponent ($-k_{obs}t$) when the initial concentrations of the limiting reagent [**1a**]₀ were doubled or halved (see Section S2 in the ESI†) confirming the first-order¹⁸ kinetic dependency on the titanium complex **1a** in the rate-limiting event. Extraction of k_{obs} from exponential decays in absorption at 495 nm afforded linear correlations against [S_2Cl_2]₀ (see Section S2 in the ESI†) confirming first-order kinetic dependency on S_2Cl_2 . The overall process {**1a** + S_2Cl_2 } is thus governed by second order kinetics, first order in both components, i.e., $-d[1a]/dt = k_1[1a][S_2Cl_2]$, with the empirical¹⁹ bimolecular rate constant, $k_1 = 320 M^{-1} s^{-1}$ at 22 °C (Table 1, entry 1).



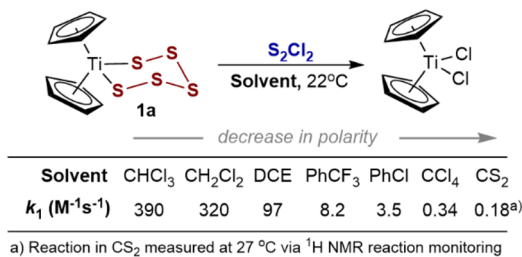


Fig. 2 Solvent effects on the empirical¹⁹ rate constant (k_1) values for the pseudo first-order reaction of **1a** with excess S₂Cl₂ at 22 °C.

Effects of solvent on the rate of reaction of S₂Cl₂ with **1a**

The ability to conduct SF-UV kinetic assays at low concentrations of **1a** allowed exploration of a range of solvents without issues relating to solubility of the reactants, intermediates, and titanocene dichloride and cycloheptasulfur products. Solvent polarity substantially affects the rate (k_1 , Fig. 2) and there is a reasonable correlation with Catalán's polarity parameters: $\log(k_1) = 49.5\{0.97 \times SA + 0.03 \times SdP\} + 0.56$; $R^2 = 0.98$; see Section 2.3 in the ESI.†²⁰ The three orders of magnitude range in rate across the series of solvents spanning from CS₂ (slowest) to CHCl₃ (fastest) is indicative of development in polar character on approach to the rate limiting transition state.

The kinetics of the reaction in CS₂ (ref. 3a) and in CCl₄, were slow enough ($k_1 = 0.18$ and 0.34 M⁻¹ s⁻¹, respectively) to allow *in situ* continuous ¹H NMR spectroscopic reaction monitoring.²¹ The NMR profiles (see ESI, Section S5†) showed no evidence for accumulation of intermediates, and remained consistent with bimolecular kinetics, *i.e.*, $-d[\mathbf{1a}]/dt = k_1[\mathbf{1a}][S_2Cl_2]$, across a range of concentrations. Overall, the analyses eliminate radical chain (mechanism V) and slow irreversible Ti-S pre-dissociation mechanisms.

Kinetics of the reactions of S₂Cl₂ with related titanacycles **1b–e** and **2a**

Reactions of S₂Cl₂ in CH₂Cl₂ with structurally related titanacycles **1b–e** and **2a** also gave bimolecular kinetics, *i.e.*, first order in both S₂Cl₂ and the titanacycle (Table 1, entries 2–6). Alkyl substitution of the cyclopentadienyl groups increases the solubility of titanocene (poly)sulfides in organic solvents.^{1a,2b} The rates of reaction of the alkylated analogues **1b–e** were all slightly slower than **1a** (Table 1, entries 2–5) with the relative rates ranging from 0.8 (**1b**, Et) to 0.3 (**1e**, *i*-Pr).

While compensating steric/electronic contributions cannot be discarded, it is reported that the donor effects of cyclopentadienyl substituents do not significantly affect the electron density on Ti in the titanapentasulfide group.²² The similar inductive effects of the alkyl substituents (*e.g.* Et, *i*-Pr, $\sigma_p = -0.15$)²³ suggest these changes to result primarily from steric hindrance. However, attempts to correlate these small differences against reported steric parameters, such as angle-descriptors for η^5 -cyclopentadienyl ligands,²⁴ did not show a clear trend (see ESI, Section S2.4†). In contrast to the negligible differences in reactivity of **1a–e**, replacing the sulfur atom

Table 1 Empirical¹⁹ bimolecular rate constants for the reaction of titanacycles **1a–e** and **2a** with S₂Cl₂ and sulfonyl chlorides **3a–c** and **4a–f** in CH₂Cl₂ at 22 °C

Entry	Titanacycle	RSCl	k_1 (M ⁻¹ s ⁻¹)	k_2 (M ⁻¹ s ⁻¹)
1	1a	S ₂ Cl ₂	3.2×10^2	— ^a
2	1b	S ₂ Cl ₂	2.4×10^2	— ^a
3	1c	S ₂ Cl ₂	2.4×10^2	— ^a
4	1d	S ₂ Cl ₂	2.0×10^2	— ^a
5	1e	S ₂ Cl ₂	0.9×10^2	— ^a
6	2a	S ₂ Cl ₂	3.4×10^4	— ^a
7	1a	3a	4.8×10^1	6.8×10^1
8	1a	3b	1.7×10^3	6.9×10^3
9	1a	3c	4.4×10^3	9.8×10^3
10	1a	4a	4.4×10^4	5.7×10^4
11	1a	4b	4.2×10^4	5.0×10^4
12	1a	4c	4.9×10^4	5.0×10^4
13	1a	4d	4.1×10^4	4.6×10^4
14	1a	4e	4.5×10^4	4.3×10^4
15	1a	4f	1.9×10^4	6.8×10^3

1	R'
a	H
b	Et
c	<i>n</i> -Pr
d	<i>n</i> -Bu
e	<i>i</i> -Pr

4	G
a	OMe
b	H
c	F
d	Cl
e	Br
f	NO ₂

^a No accumulation of an intermediate is observed in these processes, $k_2 > 10^2 k_1$.

at position 4 in the pentasulfide ring had a profound effect, with the rate of Cp₂TiS₄C(Me)₂ (**2a**) being two orders of magnitude faster (Table 1, entry 6) than with titanacycle **1a** (Table 1, entry 1). The kinetics were again first order in both components, leading to the same overall bimolecular empirical rate relationship: $-d[\mathbf{2a}]/dt = k_1[\mathbf{2a}][S_2Cl_2]$.

Kinetics of the reactions of monofunctional sulfur chlorides (RSCl) **3a–c** and **4a–f** with titanacycle **1a**

The SF-UV analyses of the reactions of monofunctional RSCl reagents **3a–c** and **4a–f** with **1a** showed distinctly different temporal UV-Vis absorption profiles (Fig. 3) to those with S₂Cl₂ (Fig. 1). The absence of isosbestic points accompanied by an increase then decay in absorbance at 495 nm indicates accumulation of a UV-Vis absorbing reactive intermediate (Fig. 3). The difference between the reactions involving the monofunctional RSCl reagents compared to S₂Cl₂ is attributed to the Cp₂TiCl(S₇Cl) intermediate generated by the latter undergoing rapid intramolecular S–S bond formation, *vide infra*.



Stopped-flow ^1H NMR spectroscopic (SF-NMR)²⁵ analysis of the reaction of **1a** with the least reactive monofunctional reagent, *N*-morpholinosulfonyl chloride **3a**, confirmed the generation of a transient species. This was tentatively assigned as the polysulfanido intermediate $\text{Cp}_2\text{TiCl}(\text{S}_6\text{R})$, consistent with Münchow and Steudel's proposal.^{7a} In this case the values for k_1 and k_2 (Table 1, entry 7) were independently determined by numerical methods fitting of both the NMR and SF-UV data (Fig. 3). The rate constants for the much more reactive RSCl reagents **3b**, **c** and **4a–f** (Table 1, entries 8–15) were extracted from numerical modelling of the UV-Vis data only, because the reactions were too fast to monitor by SF-NMR.

Each model employed multiple averaged data sets, varying $[\text{RSCl}]_0$ (see, ESI, Section S3.†) with the net absorbance assumed to arise from Beer–Lambert additivity of all species. The temporal evolution of the SF-UV data then depends on the initial reactant concentrations, the rate constants k_1 and k_2 , and the molar absorption coefficients (ϵ) of **1a**, Cp_2TiCl_2 , and $\text{Cp}_2\text{TiCl}(\text{S}_6\text{R})$. However, without being able to independently determine ϵ_{int} , we instead used the rate ratio (k_2/k_1) as a dimensionless constraint to find unique solutions to the data. These constraints were determined using analytical solutions to rapid-mixing NMR titration data²⁶ (see, ESI Section S4.2.†).

The identity of the sulfur electrophile has a major impact on the rates of reaction of **1a** with **3a–c** and **4a–f**, with k_1 and k_2 spanning three orders of magnitude (Table 1, entries 1, 7–15). The rate ratios (k_2/k_1) are also dependent on the identity of RSCl. For example **3b** is significantly more reactive towards the corresponding $\text{Cp}_2\text{TiCl}(\text{S}_6\text{R})$ intermediate than the pentasulfide

(**1a**), $k_2/k_1 = 4$. These results confirm that generation of the polysulfido intermediates in high yield from the reaction of titanacycles (**1** and **2**) with monofunctional sulfonyl chlorides is challenging.^{7a} The aryl sulfonyl chlorides (ArSCL , **4a–f**, Table 1, entries 10–15) showed the highest reactivity towards **1a**, with rate constants indicative of millisecond reaction timescales at typical concentrations employed for synthetic procedures (0.05–0.1 M).³ However, within the series, which spans classic electron-donating (*p*-OMe, **5a**) through electron-withdrawing (*p*-NO₂, **5f**) substituents, there is no meaningful correlation against Hammett substituent parameters (see ESI, Section S3.15.†). An analogous lack of correlation has previously been used to invoke concerted, $\text{S}_{\text{N}}2$ -like, mechanisms for nucleophilic substitutions at sulfur, rather than step-wise addition–elimination processes.²⁷

Activation parameters for the reactions of S_2Cl_2 and **3a** with titanacycles **1a** and **2a** in CH_2Cl_2

The kinetics of the first S–S bond forming step¹⁹ (k_1) in the reaction of **1a**, and of **2a**, with S_2Cl_2 , and both S–S bond forming steps (k_1 and k_2) in the reaction of **1a** with *N*-morpholinosulfonyl chloride **3a**, were investigated by variable temperature SF-UV kinetics. Overall, the rates are insensitive to temperature changes, showing small increases or decreases, or no change at all, depending on the identity of the titanacycle and sulfonyl chloride reagent (Fig. 4).

The rate constants for the reaction of **1a** with S_2Cl_2 remain invariant, within experimental error, between 10 and 26 °C. The reaction of S_2Cl_2 with titanacycle **2a** slightly increases in rate on

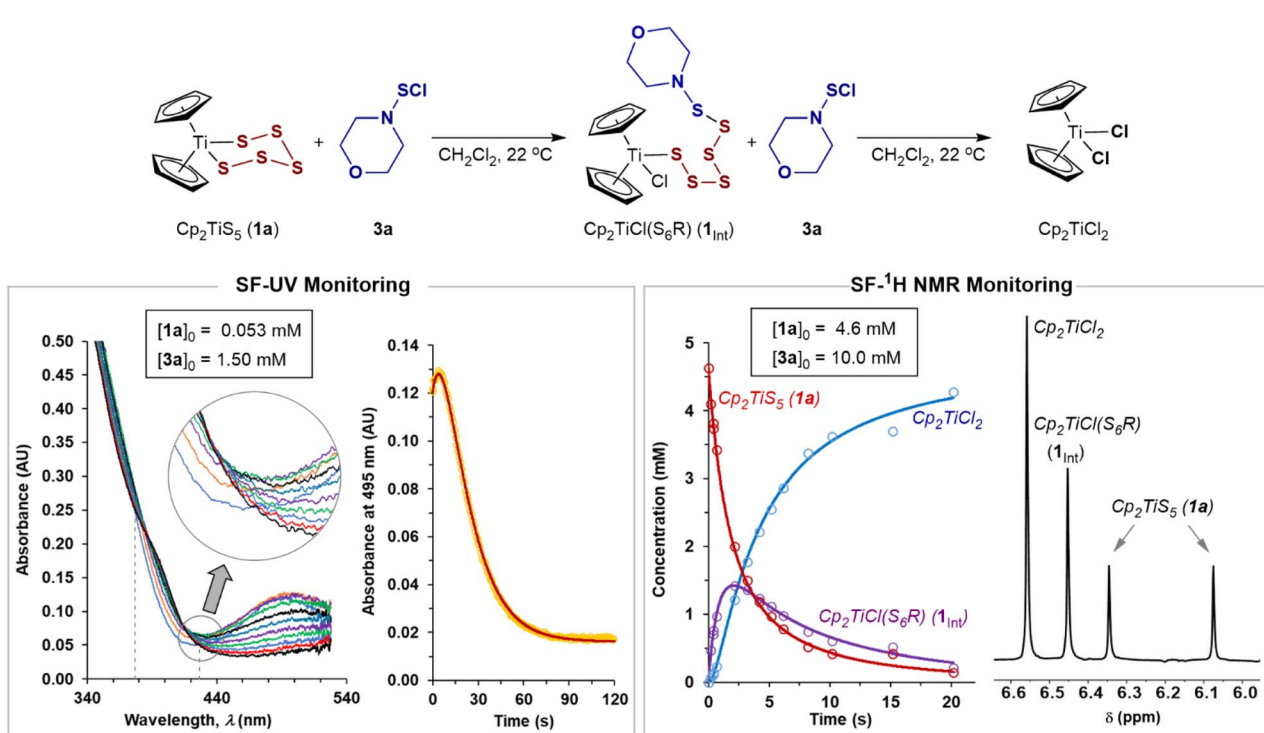


Fig. 3 Stopped-flow UV and ^1H NMR monitored evolution of the reaction of **1a** with excess sulfonyl chloride **3a**. Fitted models: solid lines; experimental data: circles.



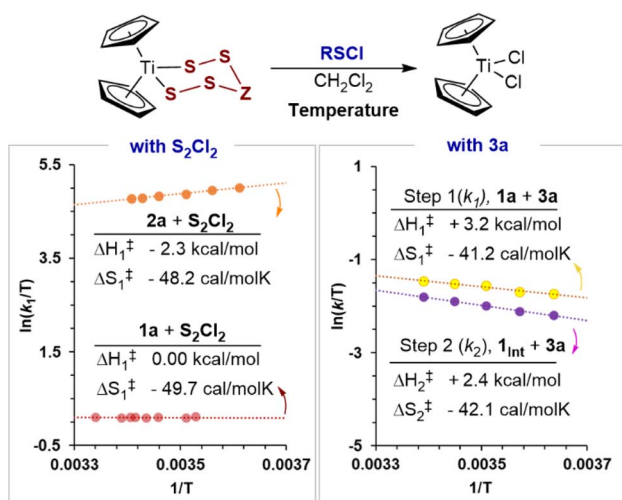


Fig. 4 Eyring analyses using process rate constants for the reaction of titanacycles with chlorosulfanes. The calculated activation parameters correspond to the microkinetic S–S bond forming events.¹⁹

cooling, ($k_{277\text{K}} \approx 1.2k_{295\text{K}}$). Conversely, both of the empirical¹⁹ rate constants (k_1 , k_2) for the reaction of **1a** with **4a** slightly decrease on cooling ($k_{275\text{K}} \approx 0.8k_{295\text{K}}$). Eyring analyses (Fig. 4)

showed all these effects arise from activation barriers that are dominated by large negative changes in entropy, with only minor enthalpic contributions (*i.e.*, $\Delta G^\ddagger/RT \approx -\Delta S^\ddagger/R$). Large negative entropies of activation can arise from significant solvent reorganisation around the transition state. However, this is more commonly observed in polar protic solvents and is unlikely to be significant in CH_2Cl_2 . Overall, the results are indicative of highly organised associative transition states which result in large losses in translational degrees of freedom in the reactants, relative to the ground state.

Computational interrogation of the reaction of S_2Cl_2 with titanacycles **1a** and **2a**

The reaction of **1a** with S_2Cl_2 was selected for initial assessment of various computational methods.²⁸ Hybrid density functionals and DLPNO-CCSD(T) failed to qualitatively describe experimental trends, likely due to a significant multideterminant character in some calculated species (see ESI, Section S11.2†). Based on these preliminary computational assays, the meta-GGA functional, $r^2\text{SCAN}$,²⁹ was chosen for further investigations.

Free energy profiles of sulfur transfer reactions of S_2Cl_2 with **1a** and **2a** are shown in Fig. 5A. Both profiles qualitatively agree with

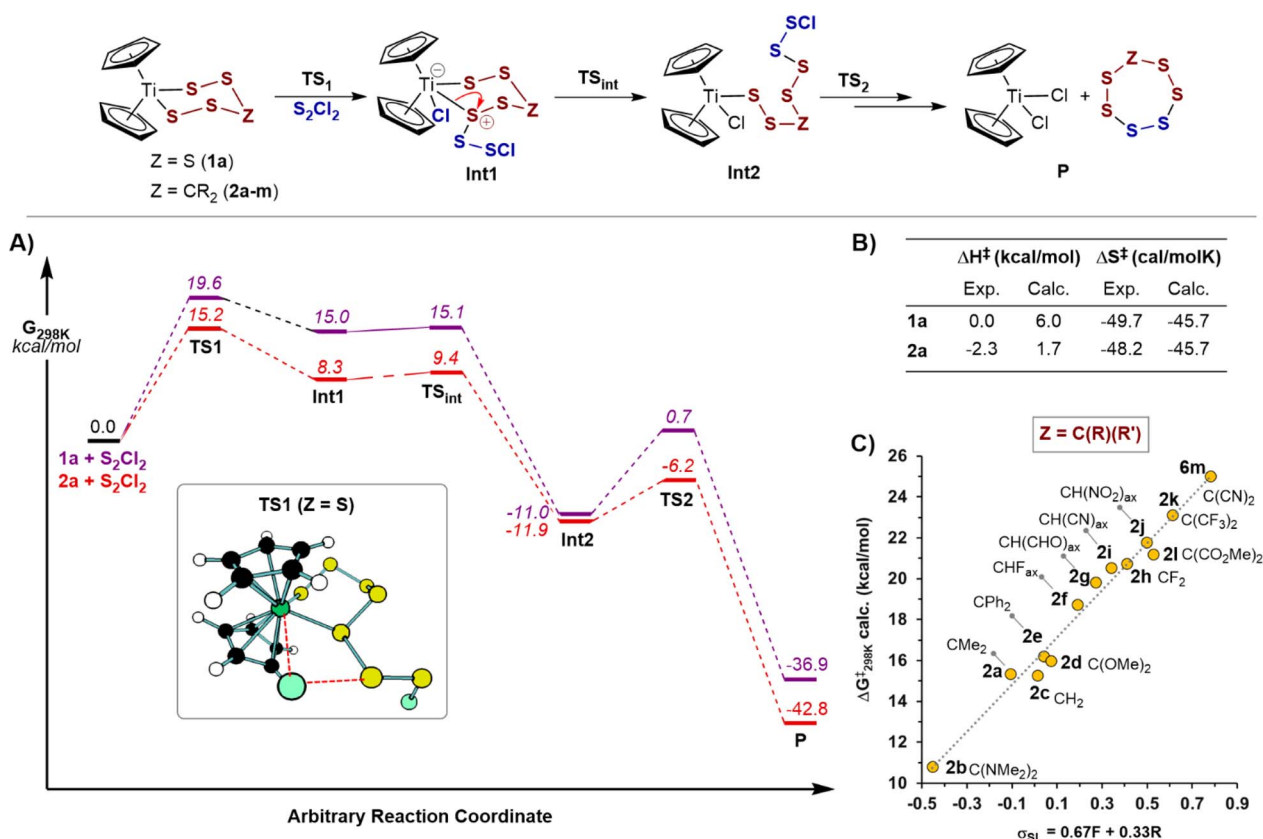


Fig. 5 (A) Computed free energy reaction profile of **1a** and **2a** with S_2Cl_2 including transition state geometry **TS1** for **1a** + S_2Cl_2 . (B) Comparison of experimental (295 K) and computed values of activation parameters of the rate limiting transition state (**TS1**) for the reaction of **1a** and **2a** with S_2Cl_2 . (C) Virtual reaction of other titanacycles $\text{Cp}_2\text{TiS}_4\text{Z}$ (**2b–m**) with S_2Cl_2 : correlation of microkinetic free energy barriers for **TS1** against Swain–Lupton substituent constants. Computational calculations performed with: $r^2\text{SCAN-D4-SMD}(\text{CH}_2\text{Cl}_2)/\text{ma-def2-QZVPP}(\text{Ti})$; $\text{ma-def2-TZVPP}(\text{C, H, S, Cl, O, N, F})/r^2\text{SCAN-3c}$, $T = 298.15\text{ K}$, $p = 1.0\text{ atm}$, $q\text{RRHO}$ cutoff = 50 cm^{-1} , $c = 1.0\text{ M}$.



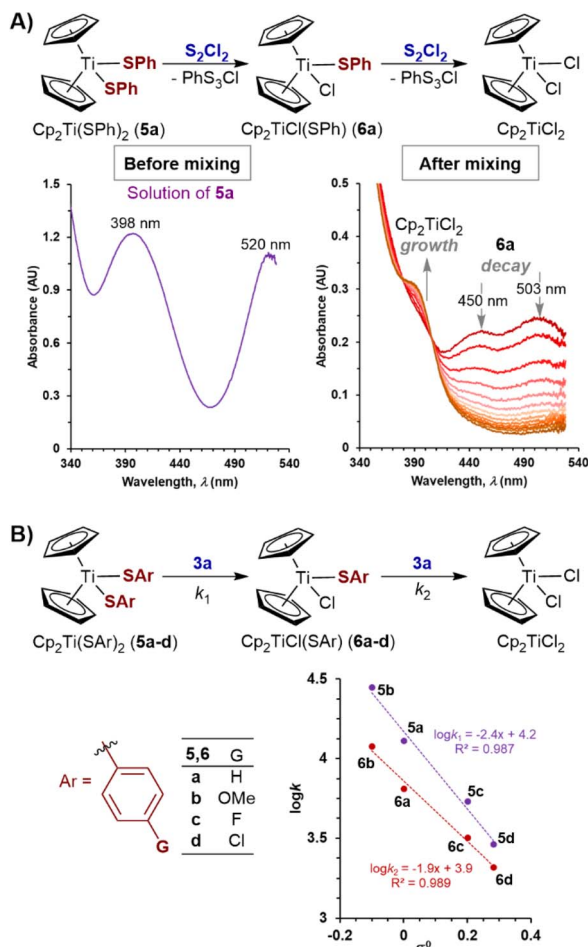


Fig. 6 (A) SF-UV monitoring of the reaction of titanocene bithiophenolate **5a** with S_2Cl_2 at 22 °C. (B) Yukawa–Tsuno linear free energy correlation for thiophenolates **5a–d** and **6a–d** in reaction with **3a**.

experimental results in that the initial sulfur transfer is rate-limiting, and that titanacycle **2a** is significantly more reactive than **1a**. Sulfur transfer from the titanocene to the sulfur chloride were found to proceed through a four-membered transition state, similar to mechanism IV, but without accompanying dissociation of the Ti–S bond. The transfer initially leads to a coordinatively saturated 18-electron titanium complex (Fig. 5, **Int1**), prior to this opening into a 16-electron polysulfide intermediate (Fig. 5, **Int2**). Other pathways explored computationally (e.g. mechanism III) were much less favourable than the process discussed above (see ESI Section S11.3[†]), and no appropriate local minimum could be found resulting from the attack of the chlorine atom of S_2Cl_2 at titanium (mechanism I).^{7a}

Comparison of the computational activation parameters for the rate controlling barriers with those determined experimentally are shown in Fig. 5B. Considering statistical corrections,¹⁹ the computational predictions are in reasonable agreement with results from experiment. The negligible changes in enthalpy and the large entropy of activation values for the reaction of **1a** ($|\Delta S_{\text{exp}}^{\ddagger} - \Delta S_{\text{calc}}^{\ddagger}| = 4.0 \text{ cal mol}^{-1} \text{ K}^{-1}$) and **2a** ($|\Delta S_{\text{exp}}^{\ddagger} - \Delta S_{\text{calc}}^{\ddagger}| = 2.5 \text{ cal mol}^{-1} \text{ K}^{-1}$) further support a concerted metathesis-like mechanism.³⁰ These results also

reinforce the conclusion that the large entropic barriers are not caused by solvent reorganisation.

The qualitative correlations found for trends in the reactions of other titanocenes (see ESI, Section S11.4[†]) prompted us to further investigate the electronic effects caused by replacing the distal sulfur in **1a** with carbon groups (**2a** and analogues **2b–m**, Fig. 5C). The microkinetic free energies of activation correlated well with inductive-weighted Swain–Lupton parameters ($\rho_{\text{SL}} = +11.5$; $R^2 = 0.98$),^{23,31} with electron-donating groups resulting in lower reaction barriers. That the correlation includes substituents of various sizes, and ground state geometries (**2b**, **2k** and **2l** have a twist-boat like geometry), suggests that steric factors, and other effects such as angle strain, only play a minor role on the relative reaction rates.

Kinetics of the reaction of S_2Cl_2 with titanocene thiophenolates **5a–d** and **6a–d**

To expand the study to acyclic titanocene sulfide di-anion surrogates, we analysed the kinetics of the reactions of thiophenolato complexes, $Cp_2Ti(SAr)_2$ (**5a–d**) and $Cp_2TiCl(SAr)$ (**6a–d**) with S_2Cl_2 , and with *N*-morpholinisulfonyl chloride **3a**. ¹H NMR spectroscopic analysis confirmed that complexes **5a** and **6a** are stable in CH_2Cl_2 solution at room temperature for at least 24 hours in the dark.

Complexes **6a–d** are however sensitive to ambient light, especially **6a** (see ESI Section S8[†]), and additional precautions were taken to avoid visible light exposure when preparing and handling their solutions.³² SF-UV analyses of the reactions of bis(thiophenolato) titanocenes **5a–d** with excess of S_2Cl_2 showed this class of substrate to be exceptionally reactive. Indeed, **5a–d** are converted into **6a–d** within the deadtime (<10 ms) of the measurement method. This is then followed by exponential decay of the monothiolates **6a–d** to Cp_2TiCl_2 (Fig. 6A). The same empirical rate constant (k_2), within experimental error, was independently determined using an isolated sample of **6a**. These features are indicative of a consecutive process for **5a–d**, with the first step being significantly faster than the second ($k_1/k_2 \geq 100$).

The high reactivity of the bis(thiophenolato) titanocenes **5a–d** is consistent with findings of Osakada and Yamamoto on the relatively slow kinetics of transmetalation of $PtClMe(COD)$ with titanocene monothiolate **6a** in THF.^{11b} However, in contrast to the second order kinetics observed for the reactions with sulfenyl chlorides studied herein, Osakada and Yamamoto found that monothiolate **6a** undergoes indirect reaction with $PtClMe(COD)$ via **5a** generated through reversible disproportionation, resulting in overall third-order kinetics.^{11b}

Direct comparison of the empirical rate constants for the reactions of titanacycles **1** and **2** with S_2Cl_2 (Table 1) against the same process for thiolate derivatives **6a–d** is not possible because the sulfenyl chloride co-product (PhS_3Cl) from the latter is highly susceptible to spontaneous desulfuration.³³ This phenomenon results in the observed decay rates of **6a–d** being the net effect of several simultaneous substitution processes. Nevertheless, similarly to titanacycles **1** and **2**, the rates of reaction of **6a** with S_2Cl_2 show a low sensitivity to temperature



($k_{281K} \approx 1.1k_{297K}$). Qualitative assessment of effects of *para*-substitution in the aromatic ring in thiophenolate derivatives **6a–d**, shows that electron-donating groups accelerate the substitution processes.³⁴

To make quantitative comparisons, SF-UV analyses of the reactions of **5a–d** with the less reactive *N*-morpholinosulfonyl chloride **3a** were conducted. The spectra showed the distinctive features of a sequential reaction: lack of isosbestic points and initial increase then decay in absorbance. Deconvolution of data showed moderate selectivity of **3a** for the bithiolate complexes ($k_1/k_2 = 1.4$ to 2.5),¹⁹ with the greater the electron donating ability of the thiolate, the higher the selectivity. Linear free energy relationships using Hammett substituent constants^{23,30} showed moderate curvature (see ESI Section S3.15†), for both experimental and computational data, despite the known correlation of nucleophilicity parameters for thiolates.³⁵ Better correlations for both steps ($k_1, \rho = -2.4$; $k_2, \rho = -1.9$) were obtained using the method of Yukawa and Tsuno,³⁶ (Fig. 6B). Both analyses indicate significant development of positive charge at the nucleophilic Ar–S–Ti sulfur atom during the transition state,³⁷ consistent with that found in computational analysis of the reaction of S_2Cl_2 with **2a–m** (Fig. 5C).

Conclusions

Using a combination of stopped-flow UV-Vis and stopped-flow NMR techniques, kinetic analyses, numerical modelling, and KS-DFT-computations, we have investigated the reactions of titanocene (poly)sulfides with a variety of sulfonyl chlorides to generate sulfur homocycles (S_n), heterocycles (E_2S_n), and polysulfanes (R_2S_n). Systematic variations in the structure of the reactants, reaction temperature, and solvent polarity have served to kinetically characterise key parameters influencing the phenomenological¹⁹ process rates. Collectively, the study provides data that supports a different mechanism to that previously proposed.^{7a} The process has all of the characteristics of a nucleophilic substitution at R–S–Cl by the titanium-bound sulfur, in a concerted, late, and metathesis-like four-membered transition state, in which chloride departure is assisted by the metal (Fig. 5).

Titanocene pentasulfide **1a** is about two orders of magnitude less reactive than the isopropylidene analogue **2a**, and about three orders of magnitude less reactive than monosulfide analogues **5a–d** and **6a–d**, to intermolecular attack of sulfonyl chlorides. In other words, the nucleophilicity of the titanium-bound sulfur is progressively attenuated by the increasing number of concatenated sulfur atoms, with the effect greatest in pentasulfide **1a**. The results also rationalise the challenges in isolating titanocene polysulfido complexes in high yields using monofunctional sulfur chlorides as electrophiles, due to consecutive processes (k_1, k_2) having similar rates. Two key outcomes from these investigations inform practical protocols for sulfur transfer from titanocenes:

(1) The low sensitivity of the process rates to temperature makes cooling useful for the preparation of thermally sensitive organic (poly)sulfides without sacrificing reactivity. Solvent polarity can also be used to tune process rates, and

incorporation of alkyl substituents on the titanocenes used to enhance solubility and thus process concentrations without a significant decrease in nucleophilicity.

(2) Titanocene thiolates undergo very rapid reactions with sulfonyl chlorides. They can be stored indefinitely as solids in the dark at -40 °C, are stable in solution for hours, and can generally be handled under air but do require protection from exposure to ambient light. Compared to the mono(thiolato) titanocenes, the bis(thiolates) are easier to access and more stable to visible light, but retain high nucleophilicity, thus making them the more practical sulfur transfer reagents.

Overall, the mechanistic features elucidated can be considered for other nucleophilic substitutions involving transition metal polysulfides, electrophiles or titanocene nucleophiles under non-aqueous conditions.

Data availability

Experimental kinetic data, NMR spectra, UV-Vis spectra, SF-methods, kinetic analyses, computational methodologies, energies, and further discussion and analysis can be found in the ESI.† Cartesian coordinates of optimised geometries are available in the OptimisedGeometries.xyz file.

Author contributions

AGD and GCL-J directed the investigation. PHHO and AGD conducted all experimental work, except for the synthesis of **1b–1f** which was carried out by GH. PHHO conducted the computational studies. PHHO, AGD, PJB and GCL-J analysed the data. All authors contributed to the preparation of the manuscript.

Conflicts of interest

There are no conflicts to declare.

Acknowledgements

We thank Eastman Chemical Company and Flexsys America L. P. for funding. We thank Dr Vera Münchow (Italy) for providing an optimised procedure for the purification of complex **2a**. We thank Sumit Chakraborty and Javier Grajeda (Eastman) for valuable discussions. We thank the University of Edinburgh Compute and Data Facility (ECDF) for access to computing resources, the EPSRC Programme Grant “Boron: Beyond the Reagent” (EP/W007517), and Royal Society (URF\R1\221133 and RG\R2\232324) for support. AGD is a Royal Society University Research Fellow.

Notes and references

- (a) A. Shaver, J. M. McCall, G. Marmolejo, F. Bottomley, E. C. Ferris and J. A. Gladysz, *Inorg. Synth.*, 1990, 59–65; (b) H. Köpf, B. Block and M. Schmidt, *Chem. Ber.*, 1968, **101**, 272–276; (c) J. Köpf and B. Block, *Chem. Ber.*, 1969, **102**, 1504–1508; (d) J. M. McCall and A. Shaver, *J. Organomet. Chem.*, 1980, **193**, C37–C39, for alternative synthetic



- procedures, see: (e) E. Samuel, *Bull. Soc. Chim. Fr.*, 1966, **11**, 3548–3564; (f) E. Samuel and C. Gianotti, *J. Organomet. Chem.*, 1976, **113**, C17–C18.
- 2 (a) D. M. Giolando and T. B. Rauchfuss, *Organometallics*, 1984, **3**, 487–489; (b) D. M. Giolando, T. B. Rauchfuss, A. L. Rheingold and S. R. Wilson, *Organometallics*, 1987, **6**, 667–675; (c) C. M. Bolinger, J. E. Hoots and T. B. Rauchfuss, *Organometallics*, 1982, **1**, 223–225; (d) C. M. Bolinger, T. B. Rauchfuss and S. R. Wilson, *J. Am. Chem. Soc.*, 1981, **103**, 5620–5621.
- 3 (a) M. Schmidt, B. Block, H. D. Block, H. Köpf and E. Wilhelm, *Angew. Chem. Int. Ed. Engl.*, 1968, **7**, 632–633; (b) R. Steudel and R. Strauss, *J. Chem. Soc., Dalton Trans.*, 1984, 1775–1777; (c) D. Dirican, N. Pfister, M. Wozniak and T. Braun, *Chem.–Eur. J.*, 2020, **26**, 6945–6963; (d) R. Steudel and B. Eckert, Solid Sulfur Allotropes, in *Elemental Sulfur and Sulfur-Rich Compounds I. Top. Current. Chem.*, ed. R. Steudel, Springer, Berlin, Heidelberg, 2003, vol. 230, pp. 1–79.
- 4 For selected examples, see: (a) R. Steudel, S. Forster and J. Albertsen, *Chem. Ber.*, 1991, **124**, 2357–2359; (b) A. Ishii and R. Yamashita, *J. Sulfur Chem.*, 2008, **29**, 303–308; (c) R. Steudel, The Synthesis of Sulfur- and Selenium-Containing Organic and Inorganic Rings from Titanocene Precursors, in *Studies in Inorganic Chemistry*, ed. R. Steudel, Elsevier, 1992, vol. 14, ch. 13, pp. 223–253.
- 5 (a) R. Steudel, M. Pridohl, J. Buschmann and P. Luger, *Chem. Ber.*, 1995, **128**, 725–728; (b) R. Steudel, K. Hassenberg, V. Münchow, O. Schumann and J. Pickardt, *Eur. J. Inorg. Chem.*, 2000, 921–928; (c) H. Schmidt and R. Steudel, *Z. Naturforsch., B: J. Chem. Sci.*, 1990, **45**, 557–558.
- 6 For selected examples of titanocene thiolate derivatives, see: (a) A. Shaver, S. Morris and A. Desjardins, *Inorg. Chim. Acta*, 1989, **161**, 11–12; (b) A. Shaver and S. Morris, *Inorg. Chem.*, 1991, **30**, 1926–1930; (c) G. Fachinetti and C. Floriani, *J. Chem. Soc., Dalton Trans.*, 1974, 2433–2436; (d) H. Köpf and H. Schmidt, *Z. Anorg. Allg. Chem.*, 1965, **340**, 139–145; (e) D. Taher, S. Klaib, T. Stein, M. Korb, G. Rheinwald, A. Ghazzy and H. Lang, *Polyhedron*, 2018, **148**, 70–75; (f) N. W. Alcock, H. J. Clase, D. J. Duncalf, S. L. Hart, A. McCamley, P. J. McCormack and P. C. Taylor, *J. Organomet. Chem.*, 2000, **605**, 45–54; (g) See also ref. 11.
- 7 (a) V. Münchow and R. Steudel, *Eur. J. Inorg. Chem.*, 2004, 718–725; (b) R. Steudel, O. Schumann, J. Buschmann and P. Luger, *Angew. Chem., Int. Ed.*, 1998, **37**, 492–494; (c) N. Takeda, N. Tokitoh and R. Okazaki, Polysulfido Complexes of Main Group and Transition Metals, in *Elemental Sulfur and Sulfur-Rich Compounds II. Top. Current. Chem.*, ed. R. Steudel, Springer, Berlin, Heidelberg, 2003, vol. 231, pp. 153–202.
- 8 For a review on organic polysulfane chemistry, see: R. Steudel, *Chem. Rev.*, 2002, **102**, 3905–3946.
- 9 For examples of other reagents for the regulated synthesis of disulfides and polysulfides ($n > 2$) see: (a) X. Xiao, M. Feng and X. Jiang, *Angew. Chem. Int. Ed. Engl.*, 2016, **55**, 14121–14125; (b) X. Xiao, J. Xue and X. Jiang, *Nat. Commun.*, 2018, **9**, 2191; (c) J. Xue and X. Jiang, *Nat. Commun.*, 2020, **11**, 4170; (d) Q. Yu, L. Bai and X. Jiang, *Angew. Chem., Int. Ed.*, 2023, **62**, e202314379, and references therein.
- 10 For a kinetic study of the relatively slow reaction of Cp₂TiS₅ with dimethyl acetylenedicarboxylate alkynes, see: (a) C. M. Bollinger and T. B. Rauchfuss, *Inorg. Chem.*, 1982, **21**, 3947–3954, for related processes with Zn(II)-reagents; (b) R. J. Pafford, J.-H. Chou and T. B. Rauchfuss, *Inorg. Chem.*, 1999, **38**, 3779–3786; (c) M. Ballesteros and E. Y. Tsui, *Dalton Trans.*, 2020, **49**, 16305–16311.
- 11 For kinetic studies on the the relatively slow transmetallation of sulfur from titanocenes into Pt(II) complexes, see: (a) K. Osakada, Y. Kawaguchi and T. Yamamoto, *Organometallics*, 1995, **14**, 4542–4548; (b) K. Osakada, T. Oshoda and T. Yamamoto, *Bull. Chem. Soc. Jpn.*, 2000, **73**, 923–930.
- 12 For examples of studies of substitutions with sulfur compounds at sulfenyl-chlorides, see: C. G. Moore and M. Porter, *J. Chem. Soc.*, 1958, 2888–2904. , note 584.(b) C. G. Moore and M. Porter, *Tetrahedron*, 1960, **9**, 58–64; (c) F. Pietra and D. Vitali, *J. Chem. Soc. B*, 1970, 623–625.
- 13 (a) E. Ciuffarin and A. Fava, Nucleophilic Substitution at Sulfur, in *Progress in Physical Organic Chemistry*, ed. A. Steitwieser Jr and R. W. Taft, John Wiley and Sons, Inc., 1968, vol. 6, ch. 2, pp. 81–110; (b) J. L. Kice, Nucleophilic Substitution at Different Oxidation States of Sulfur, in *Progress in Inorganic Chemistry*, ed. J. O. Edwards, John Wiley and Sons, Inc., 1972, vol. 17, pp. 148–206; (c) S. Oae, in *Organic Sulfur Chemistry: Structure and Mechanism*, ed. J. T. Doi, CRC Press Taylor & Francis Group, Florida, 1st edn, 1991, vol. 1, ch. 4, pp. 119–181.
- 14 For a review on computational analysis of S_N2-reactions, see: T. A. Hamlin, M. Swart and F. M. Bickelhaupt, *ChemPhysChem*, 2018, **19**, 1315–1330.
- 15 For selected examples of radical chain reactions using sulfenyl chlorides proceeding via thiyl radicals as carriers, see: (a) D. D. Tanner, N. Wada and B. G. Brownlee, *Can. J. Chem.*, 1973, **51**, 1870–1879; (b) J. F. Harris Jr, *J. Org. Chem.*, 1966, **31**, 931–935; (c) R. G. Guy and I. Pearson, *J. Chem. Bull. Soc. Jpn.*, 1977, **50**, 541–542.
- 16 For selected examples on the role of titanocene(III) in halogen abstraction, see: (a) G. Hersant, M. B. S. Ferjani and S. M. Bennett, *Tetrahedron Lett.*, 2004, **45**, 8123–8126; (b) Y. Qian, G. Li, X. Zheng and Y.-Z. Huang, *Synlett*, 1991, 489–490; (c) X. Wu, W. Hao, K.-Y. Ye, B. Jiang, G. Pombar, Z. Song and S. Lin, *J. Am. Chem. Soc.*, 2018, **140**, 14836–14843, titanocene(III) chloride can also react with disulfides delivering sulfur-centered radical species; (d) R. S. P. Coutts, J. R. Surtees, J. M. Swan and P. C. Wailes, *Aust. J. Chem.*, 1966, **19**, 1377–1380.
- 17 ¹H NMR spectra of complex **1a** show it exists as a mixture of two chair-conformers with inversion barriers reported to be $\Delta G_{298.15}^{\ddagger} = 76.3 \text{ kJ mol}^{-1}$ ($k = 1.65 \text{ s}^{-1}$; $t_{0.5} = 0.42 \text{ s}$) based on VT-NMR line-shape analyses: (a) E. W. Abel, M. Booth and K. G. Orrell, *J. Organomet. Chem.*, 1978, **160**, 75–79, while the inversion has been justified by ‘the usual chair-to-chair’ interconversion, evidence against a ring-opening pathway has not been provided; (b) Upon UV-irradiation,



- a homolytic pathway is favoured over heterolytic Ti-S cleavage: A. E. Bruce, M. R. M. Bruce and D. R. Tyler, *J. Am. Chem. Soc.*, 1984, **106**, 6660–6664, see also: ; (c) M. R. M. Bruce, A. Kenter and D. R. Tyler, *J. Am. Chem. Soc.*, 1984, **106**, 639–644.
- 18 This eliminates the possibility of a higher order dependency on **1a** exhibiting pseudo first-order kinetics via self/autocatalysis. The latter situation is detected by the exponent ($-k_i$) to the first-order decay being dependent on the initial reactant concentration. For an example of this, see: P. A. Cox, M. Reid, A. G. Leach, A. D. Campbell, E. J. King and G. C. Lloyd-Jones, *J. Am. Chem. Soc.*, 2017, **139**, 13156–13165.
- 19 In some cases, the possibility of degenerate pathways for one or more specific steps in the reaction mean that the phenomenological process rates lead to empirical constants (k_1 , k_2) that differ from the microkinetic rate constants. For example, in the case of $\{\mathbf{1a} + \text{S}_2\text{Cl}_2\}$ the presence of two identical Ti-S bonds in **1a** and two identical S-Cl bonds in S_2Cl_2 results in four degenerate pathways for the first S-S cleavage, and thus statistical corrections (in this specific case, $k_1/4$) are required for calculation of activation parameters; see Section S.11.2 in the ESI† for further discussion. The statistical effects must also be considered when calculating selectivity for two microkinetic steps from the relative rate constants (k_1/k_2) for the two steps in the phenomenological process, and *vice versa*.
- 20 (a) J. Catalán, *J. Phys. Chem. B*, 2009, **113**, 5951–5960; (b) There was not a meaningful correlation of the process rate constants with the ET30 scale, dipole moment or dielectric constant of various solvents (see the ESI Section S2.3†).
- 21 Y. Ben-Tal, P. J. Boaler, H. J. A. Dale, R. E. Dooley, N. A. Fohn, Y. Gao, A. Garcia-Dominguez, K. M. Grant, A. M. R. Hall, H. L. D. Hayes, M. M. Kucharski, R. Wei and G. C. Lloyd-Jones, *Prog. Nucl. Magn. Reson. Spectrosc.*, 2022, **129**, 28–106.
- 22 (a) A. Shaver and J. M. McCall, *Organometallics*, 1984, **12**, 1823–1829; (b) G. Tainturier and B. Gautheron, *Phosphorus Sulfur*, 1988, **36**, 11–14; (c) The tert-butyl-Cp analogue of **1a** was not explored but this substituent is anticipated to have a negligible inductive effect on the reactivity.
- 23 C. Hansch, A. Leo and R. W. Taft, *Chem. Rev.*, 1991, **91**, 165–195.
- 24 N. J. Coville, M. S. Loonat, D. White and L. Carlton, *Organometallics*, 1992, **11**, 1082–1090.
- 25 (a) R. Wei, A. M. R. Hall, R. Behrens, M. S. Pritchard, E. J. King and G. C. Lloyd-Jones, *Eur. J. Org. Chem.*, 2021, 2331–2342; (b) H. J. A. Dale, G. R. Hodges and G. C. Lloyd-Jones, *J. Am. Chem. Soc.*, 2023, **145**, 18126–18140.
- 26 A competition of **1a** and **2a** for substoichiometric quantities of S_2Cl_2 added by microsyringe to their solution in a 5 mm NMR tube gave rate constant ratios that differed by two orders of magnitude to those obtained using efficient rapid mixing by flow methods, see Section S7 in the ESI†
- 27 (a) C. Brown and D. R. Hogg, *Chem. Commun.*, 1967, 38–39; (b) For a full discussion on concerted versus associative-dissociative pathways in $\text{S}_{\text{N}}2$ at sulfur, see ref. 12b.
- 28 Computations were performed using ORCA software, F. Nesse, *Wiley Interdiscip. Rev.: Comput. Mol. Sci.*, 2022, **12**, e1606.
- 29 (a) J. W. Furness, A. D. Kaplan, J. Ning, J. P. Perdew and J. Sun, *J. Phys. Chem. Lett.*, 2020, **11**, 8208–8215; (b) S. Grimme, A. Hansen, S. Ehlert and J.-M. Mewes, *J. Chem. Phys.*, 2021, **154**, 064103.
- 30 For examples of concerted σ -bond methatheses with similar activation parameters see: R. Waterman, *Organometallics*, 2013, **32**, 7249–7263.
- 31 For the para-fluorine substituent we used the value of $\sigma_{\text{p}} = 0.15$, which is better parameterized for reactions in anhydrous organic solvents: (a) A. T. Shulgin and A. W. Baker, *Nature*, 1958, **182**, 1299; (b) T. J. A. Corrie, L. T. Ball, C. A. Russell and G. C. Lloyd-Jones, *J. Am. Chem. Soc.*, 2017, **139**, 245–254.
- 32 For studies on the behaviour of titanocene (poly)sulfides on irradiation with UV-light, see: (a) H. Kunkely and A. Vogler, *Z. Naturforsch., B: J. Chem. Sci.*, 1998, **53**, 22; (b) Ref. 17b, which reports on the higher sensitivity of these thiolate complexes to irradiation compared to Cp_2TiS_5 .
- 33 A previous report in polysulfane synthesis involving aryl polysulfane chlorides (ArS_xCl) as intermediates stated that they ‘must be protected from moisture and pure starting materials must be used since the intermediates and end products were not purified by distillation due to their very considerable tendency to disproportionate: H. J. Langer and J. B. Hyne, *Can. J. Chem.*, 1973, **51**, 3403–3411.
- 34 The reactions of titanocene thiophenolate derivatives **5a-d** and **6a-d** with ArSCl reagents were too fast to measure using the SF-UV equipment available. This shows these titanocene thiophenolates are much more nucleophilic than the corresponding thiophenols, ArSH . For the kinetics of the latter, see: A. García-Domínguez, N. M. West, R. T. Hembre and G. C. Lloyd-Jones, Thiol Chlorination with *N*-Chlorosuccinimide: HCl-Catalyzed Release of Molecular Chlorine and the Dichotomous Effects of Water, *ACS Catal.*, 2023, **13**, 9487–9494.
- 35 P. M. Jüstel, C. D. Pignot and A. R. Ofial, *J. Org. Chem.*, 2021, **86**, 5965–5972.
- 36 (a) Y. Yukawa and Y. Tsuno, *Bull. Chem. Soc. Jpn.*, 1959, **32**, 971–981; (b) Y. Yukawa, Y. Tsuno and M. Sawada, *Bull. Chem. Soc. Jpn.*, 1966, **39**, 2274–2286.
- 37 The mechanistic similarities of the reactions of **5a-d** and **6a-d** to the analogous reactions of titanacycles **1a** and **2a**, as well as reasonable correlations with computation (see ESI†) argues against a change in mechanism across the series.

